Author Manuscript

Author Manuscript

Author Manuscript

Author Manuscript

HHS Public Access

Author manuscript

*Cell Rep*. Author manuscript; available in PMC 2016 February 10.

Published in final edited form as:

*Cell Rep*. 2015 March 31; 10(12): 1957–1966. doi:10.1016/j.celrep.2015.03.038.

# UHRF1 Contributes to DNA Damage Repair as a Lesion Recognition Factor and Nuclease Scaffold

**Yanyan Tian**[1], **Manikandan Paramasivam**[2], **Gargi Ghosal**[1], **Ding Chen**[4], **Xi Shen**[1], **Yaling huang**[1], **Shamima Akhter**[3], **Randy Legerski**[3], **Junjie Chen**[1], **Michael M Seidman**[2], **Jun Qin**[4], and **Lei Li**[1,3]

Lei Li: leili@mdanderson.org

[1]Department of Experimental Radiation Oncology, the University of Texas M. D. Anderson Cancer Center, Houston, TX

[2]Laboratory of Molecular Gerontology, National Institute of Aging, National Institutes of Health

[3]Department of Genetics, the University of Texas M. D. Anderson Cancer Center, Houston, TX

[4]Department of Biochemistry, Baylor College of Medicine, Houston, TX

## Summary

We identified UHRF1 as a binding factor for DNA interstrand crosslink (ICL) lesions through affinity purification of ICL-recognition activities. UHRF1 is recruited to DNA lesions *in vivo* and binds directly to ICL-containing DNA. UHRF1-deficient cells display increased sensitivity to a variety of DNA damages. We found that loss of UHRF1 led to retarded lesion processing and reduced recruitment of ICL repair nucleases to the site of DNA damage. UHRF1 interacts physically with both ERCC1 and MUS81, two nucleases involved in the repair of ICL lesions. Depletion of both UHRF1 and components of the Fanconi anemia pathway resulted in increased DNA damage sensitivity compared to defect of each mechanism alone. These results suggest that UHRF1 promotes recruitment of lesion-processing activities via its DNA damage recognition affinity and functions as a nuclease recruitment scaffold in parallel to the Fanconi anemia pathway.

## Introduction

The DNA interstrand crosslink (ICL) is a complex DNA lesion arising from a variety of extrinsic and intrinsic bifunctional alkylating agents. ICL-inducing agents exhibit profound cytotoxicity and are among the most widely used chemotherapy drugs (McHugh et al., 2001). Deficiencies in repairing DNA ICLs have severe pathological consequences as highlighted by the recessively inherited cancer prone disease, Fanconi anemia (FA) (D'Andrea, 2010; Kim and D'Andrea, 2012).

Repair of DNA ICLs is accomplished by two distinct pathways. The replication-dependent pathway operates primarily during S phase, initiated by replication fork encountering with an ICL. Since the formation of an ICL compromises both strand of the double helix, error-

Correspondence to: Lei Li, leili@mdanderson.org.

Author Manuscript Author Manuscript Author Manuscript Author Manuscript

free repair most likely involves homologous recombination with the undamaged sister chromatid upon formation of DNA strand breaks (Knipscheer et al., 2009; Long et al., 2011). Consistently, defects in homologous recombination factors such as Brca2, Rad51C, and BACH1 render cells sensitive to crosslinking agents. On the other hand, ICLs in G1/G0 phases of the cell cycle or during early S phase utilize a recombination-independent mechanism involving the combined actions of the nucleotide excision repair and lesion bypass synthesis (Sarkar et al., 2006; Williams et al., 2012; Zheng et al., 2003).

A key step in ICL repair is the loading of the appropriate nucleases to the damaged site to achieve the initial incision and unhooking of an ICL. Genetic and biochemical studies have identified several nucleases including ERCC1-XPF, MUS81-EME1, SNM1A (Hodskinson et al., 2014; Wang et al., 2011) in the nucleolytic processing of ICLs. These structural-specific endonucleases act at different stages of ICL removal, generating intermediates of single or double strand breaks adjacent to the ICL lesion, and allowing subsequent lesion bypass and homologous recombination to take place (Bhagwat et al., 2009; Hodskinson et al.). However, the molecular mechanisms directing the recruitment of nucleases to the damaged sites are poorly understood. The main function of the FA pathway is presumed to be the loading of lesion processing nucleases via FAND2/I monoubiquitination-mediated regulation of the SLX4/FANCP nuclease scaffold (Guervilly et al.; Muñoz et al., 2009; Ouyang et al.; Smogorzewska et al., 2010; Stoepker et al., 2011; Svendsen et al., 2009). It is unclear, however, whether ICL-processing activities can be recruited through other mechanisms.

UHRF1 (Ubiquitin-like with PHD and ring-finger domain 1) is a multi-domain protein important for the maintenance of cytosine methylation. It recognizes specific forms of histone modifications and DNA hemimethylation (Liu et al., 2013; Nishiyama et al., 2013) and facilitates the recruitment of Dnmt1 to catalyze the methylation reaction on hemimethylated CpG motifs. As expected, cells defective in UHRF1 have reduced amplitude and site accuracy of DNA methylation (Bostick et al., 2007). However, UHRF1 loss also causes cellular sensitivity to DNA damaging agents (Muto et al., 2002). Mechanistic insights on this unexpected phenotype are unknown. In this report, we identified UHRF1 as an ICL-binding protein through an unbiased affinity purification of lesion-binding activities. Analyses of UHRF1-deficient cells revealed an unanticipated defect in lesion processing. We found that URHF1 interacts with lesion processing nucleases ERCC1 and MUS81 and may serve as a recruitment factor for the repair of DNA lesions. These results suggest a UHRF1-dependent mechanism of directing structure-specific nucleases to the site of DNA damage.

## Results

### Identification of UHRF1 as an ICL-binding protein

To isolate proteins that bind to DNA ICLs, we designed a 120-bp oligonucleotide duplex, which has two TA motifs for the formation of site-specific psoralen-based ICLs (Figure 1A and Figure S1A). Upon psoralen/UVA treatment, crosslinked oligos (XL) were purified, end-labeled with biotin, and used as the crosslinked substrate for ICL-affinity purification. A control substrate (Ctrl) was generated in parallel without the addition of AMT. The

Author Manuscript Author Manuscript Author Manuscript Author Manuscript

crosslinked and control substrates were attached to streptavidin beads and incubated with HeLa nuclear extracts. Tightly bound proteins were eluded and subjected to mass spectrometry analyses. The amount of each protein bound to crosslinked substrate was normalized to that of the control substrate to yield a ratio (XL/Ctrl) as a reflection of its affinity to the ICL. As shown in Figure 1B, we found that the UHRF1 protein is highly enriched by the crosslinked substrate.

To exclude the possibility that the identification of UHRF1 was biased toward sequence composition, we repeated the pull down experiment with a second set of crosslinked and control substrates (Substrate B, Figure S1A) in which only the two TA motifs and their relative positions are identical to the original substrate (Substrate A). UHRF1 was again identified as the top candidate, suggesting that binding of UHRF1 to ICL-containing DNA does not rely on the sequence context of the ICL substrates.

To test whether UHRF1 binds to ICLs *in vivo*, laser-localized psoralen ICLs were introduced into the nuclei of U2OS cells (Muniandy et al., 2009) expressing GFP-UHRF1. Beginning at 30 seconds after ICL induction, GFP-UHRF1 accumulated at the ICL track and appeared to peak around 8 minutes (Figure 1C & 1D). This result indicates that UHRF1 is specifically enriched at the sites of ICL lesions and its recruitment is an early event in ICL response when compared to the recruitment of FANCA (Yan et al., 2012).

Next, we performed the eChIP assay (Shen et al., 2009) with psoralen- or cisplatin-derived ICL lesions. The eChIP substrate contains a defined psoralen ICL positioned 488 bases downstream of the EBV replication origin (Figure S1B and 1C). Therefore, protein recruitment to the site of the ICL can be analyzed in the absence or presence of DNA replication to determine whether a blocked replication fork is required. We found that the presence of a single-defined psoralen ICL yielded significant UHRF1 enrichment onto the crosslinked substrate (Figure 1E). The enrichment was not significantly increased when substrate replication was enabled in the 293EBNA cells, suggesting that stalled replication fork is not essential for UHRF1 binding to the ICL. The increased UHRF1 recruitment in both control and ICL substrates mostly likely reflect a replication-coupled enrichment of UHRF1 (Nishiyama et al., 2013). Consistently, eChIP substrate containing randomly introduced cisplatin ICLs showed a significant enrichment of UHRF1 in a dose-dependent manner in both replicated and unreplicated sites of ICLs (Figure 1F). These results suggested that UHRF1 is recruited to sites of DNA ICLs *in vivo*.

## UHRF1 binds directly to ICLs through the SRA domain

Although UHRF1 is shown to be associated with ICLs in nuclear extracts and *in vivo*, such association could be mediated by other factors. We therefore tested whether UHRF1 directly bound DNA ICLs. An MBP-UHRF1 recombinant protein was purified via amylose beads and incubated with DNA containing psoralen- or cisplatin-induced ICLs. As shown in Figure 2A, MBP-UHRF1 retained specifically crosslinked DNA but not control DNA, whereas MBP alone showed no detectable binding to either DNA probes.

We further validated the affinity of UHRF1 to ICL substrates in a competition assay. Immobilized MBP-UHFR1 fusion protein was pre-incubated with $^{32}$P-labeled

Author Manuscript Author Manuscript Author Manuscript Author Manuscript

oligonucleotide containing psoralen or cisplatin ICLs, followed by the addition of increasing amounts of unlabeled ICL-containing or control oligo (Figure 2B & 2C). The results showed that the ICL-containing oligonucleotide was much more efficient in competing for UHRF1 binding than the control. These results demonstrated that UHRF1 exhibits direct affinity for DNA ICLs.

UHRF1 contains five conserved motifs that include UBL, tandem TUDOR, PHD, SRA, and RING domains (Figure 2D). To determine whether the ICL-binding activity could be localized to a specific region or domain(s), we generated five truncation mutants. Each mutant has one of the five conserved domains removed. MBP-fusion proteins of each mutant were purified and tested in the ICL pull-down assay using psoralen or cisplatin ICL DNA. As shown in Figure 2E, only deletion of the SRA domain completely abolished UHRF1 binding to ICL containing DNA, indicating that the SRA domain is most critical for UHRF1's ability to recognize DNA crosslinking lesions.

## Loss of UHRF1 function leads to DNA damage sensitivity

The association of UHRF1 with ICL lesions suggested that it may play a role in cellular response to ICLs. To test this premise, we established a UHRF1 conditional allele in the HCT116 background via somatic cellular targeting (Figure S2A). Although homozygous deletion of UHRF1 leads to severe proliferation defect (Figure S2B–D), we obtained two independent hypomorphic mutants (UHRF1$^{-/Neo}$-1 and UHRF1$^{-/Neo}$-2) in which one UHRF1 allele was inactivated and the other was rendered hypomorphic by the insertion of a Neo$^{R}$ cassette upstream of exon 4. As a result, both hypomorphic mutants express UHRF1 protein at significantly reduced levels compared to wild type *UHRF1*$^{+/+}$ cells, but maintain normal growth characteristics.

We next analyzed UHRF1$^{-/Neo}$-1 and UHRF1$^{-/Neo}$-2 mutants for their sensitivity to DNA damage exposure. As shown in Figure 3A–C, both hypomorphic mutants displayed increased sensitivity to mitomycin C, UV, or Pso-UVA treatments. Complementation of both mutants with wild type UHFR1 restored cell survival to that of the wild type HCT116 cells. Knockdown of UHRF1 in 293T and HeLa cells also significantly increased their sensitivity to mitomycin C and UV (Figure S2E–F). When compared to FANCL or SLX4 *null* mutants, UHRF1 hypomorphic cells are considerably less sensitive (Figure 5B–C). Compared to isogenic FANCM$^{-/-}$ and FAAP24$^{-/-}$ mutants, however, the UHRF1 hypomorphic mutants displayed similar sensitivities to mitomycin C (Figure S2G). These result suggested that UHRF1 is functionally involved in cellular resistance against DNA damage.

As an important factor in maintaining DNA cytosine methylation (Bostick et al., 2007), the UHRF1 RING domain-dependent E3 ligase activity has been found essential for the recruitment of DNMT1 and subsequent replication of cytosine methylation patterns (Nishiyama et al., 2013). When two UHRF1 E3 ligase mutants, C724A and H741A (Jenkins et al., 2005), were used to complement the UHRF1$^{-/Neo}$ cells, the DNA damage resistance was largely restored (Figure S2H). This result indicated that disruption of methylation maintenance was unlikely the primary cause for the damage sensitivity phenotype and that UHRF1 may have functions directly linked to the DNA damage response.

Author Manuscript Author Manuscript Author Manuscript Author Manuscript

The DNA damage sensitive phenotype suggests that UHRF1 mutant cells may be deficient in the removal of ICL lesions efficiently, resulting in a higher level of residue damage and decreased cell survival. Thus we analyzed γH2AX foci formation in $UHRF1^{-/Neo}$ and $UHRF1^{+/+}$ cells exposed to mitomycin C. Under unperturbed growth conditions, $UHRF1^{-/Neo}$ cells exhibit a higher percentage of γH2AX foci-positive nuclei (Figure 3D). This result suggests that cells lacking UHRF1 function indeed accumulate DNA damage. Upon mitomycin C treatment, however, both the $UHRF1^{-/Neo}$-1 and $UHRF1^{-/Neo}$-2 mutants showed a markedly reduced γH2AX foci formation when compared with wild type $UHRF1^{+/+}$ cells, especially at later time points (12 and 24 hours) (Figure 3E). Similarly, Immunoblotting of γH2AX (Figure 3F) also confirmed the attenuated onset of γH2AX induction upon DNA damage and a higher level of basal level γH2AX in the absence of exogenous DNA damage. To further validate these results, we analyzed 53BP1 foci formation in $UHRF1^{-/Neo}$ mutants exposed to mitomycin C. Consistent with the γH2AX results, mitomycin C-mediated 53BP1 foci formation also decreases in *$UHRF1^{-/Neo}$* mutant cells (Figure S3A, B). These results suggest that UHRF1 plays a role in the repair of both endogenous and exogenous lesions.

## UHRF1 function is involved in the recruitment of ICL damage-processing activities

Because formation of DNA strand breaks is a primary signal that triggers the accumulation of γH2AX and 53BP1, attenuated foci formation in UHRF1-deficient cells may reflect a potential lack of ICL processing that creates DNA strand breaks. Therefore, we tested the premise that impaired recruitment of lesion-processing nuclease activities contributes to the diminished induction of γH2AX and 53BP1 foci and to the DNA damage sensitivity phenotype from UHRF1-deficiency. First, we asked whether UHRF1 interacts directly with ERCC1-XPF or MUS81-EME1, two structure-specific endonucleases which are required in processing ICL lesions. As shown by co-immunoprecipitation of both tagged and endogenous proteins (Figure 4A–C, Figure S3B), UHRF1 interacts with both ERCC1/XPF and MUS81/EME1. Moreover, recombinant MBP-UHRF1 was able to pulldown MUS81 and ERCC1 from HeLa nuclear extract. An N-terminal UHRF1 truncation lacking the SRA and RING domains disrupted the association with both ERCC1 and MUS81, whereas a C-terminal truncation retaining these domains was able to bind MUS81 and ERCC1 (Figure 4D). Together, these results suggest a direct interaction between UHRF1 and ICL-processing nucleases.

Both ERCC1-XPF and MUS81-EME1 are known to be associated with a common scaffold protein, SLX4/FANCP (Fekairi et al., 2009; Munoz et al., 2009; Svendsen et al., 2009). We asked whether the observed interactions are mediated by SLX4. To this end, we generated a HeLa SLX4 *null* mutant and examined the interactions between UHRF1 and the two nucleases by co-immunoprecipitation (Figure 4E). We found that deletion of SLX4 does not abolish the interactions, suggesting that binding of UHRF1 to the lesion-processing nucleases is independent of SLX4. Consistently, reciprocal IP between Myc-SLX4 and SFB-UHRF1 showed no detectable interaction between the two proteins (Figure 4F).

Given UHRF1's lesion-binding affinity and its direct interactions with lesion-processing nucleases, a likely function for UHRF1 in DNA damage response may be to recruit lesion-

Author Manuscript Author Manuscript Author Manuscript Author Manuscript

processing nucleases to the site of damage. We tested this notion by eChIP in the *UHRF1*$^{-/Neo}$ hypomorphic mutant cells. As shown in Figure 4G, enrichment of Mus81 onto cisplatin-adducted DNA substrate is significantly reduced in both UHRF1 mutants, compared with the parental *UHRF*$^{+/+}$ cells. Similarly, enrichment of ERCC1 is also reduced in the *UHRF1*$^{-/Neo}$ hypomorphic mutant cells (Figure 4H), suggesting a role for UHRF1 in the processing of ICL lesions by recruiting structure-specific endonucleases.

### UHRF1 function in DNA damage response is not redundant with the FA pathway

Although UHRF1 interacts with ERCC1 and MUS81 independently of SLX4, it is unclear whether UHRF1 is functionally distinct from the FA pathway. To address this question, we tested whether activation of the FA pathway is compromised in the UHRF1-deficient cells (Figure 5A). We found that both UHRF1 hypomorphic mutants exhibited mitomycin C-induced FANCD2 monoubiquitination similar to wild-type controls, suggesting that activation of the FA pathway is not significantly affected by UHRF1 depletion.

To functionally determine whether UHRF1's role in DNA damage response is distinct from the FA mechanism, we knocked down UHRF1 in SLX4$^{-/-}$ HeLa cells and analyzed clonogenic survival against cisplatin (Figure 5B, Figure S4A). Compared to cells lacking UHRF1 or SLX4 alone, the combined loss of UHRF1 and SLX4 acquired additional hypersensitivity to DNA damage, suggesting that the damage repair function of UHRF1 is parallel to that of SLX4.

To substantiate this result further, *FANCL*$^{-/-}$ cells constructed in HeLa background were depleted of UHRF1 via shRNA knockdown. Clonogenic survival indicated that UHRF1 knockdown in HeLa cells yielded increased sensitivity to mitomycin C, although less profound than FANCL knockout cells. However, UHRF1 knockdown in *FANCL*$^{-/-}$ HeLa cells produced enhanced sensitivity to mitomycin C (Figure 5C, Figure S4B). Consistently, UHRF1 knockdown in *FANCL*$^{-/-}$ HCT116 cells also rendered additional cell killing by mitomycin C (Figure 5D). These results suggest that UHRF1 provides ICL repair functions independent of the FA pathway components, most likely through its lesion-binding capability and recruitment of lesion-processing nucleases.

## Discussion

Each type of DNA damage, such as bulky adducts, mismatches, and DNA double strand breaks, is recognized by a lesion-specific damage-binding protein to initiate the repair process. In the case of DNA ICLs, it has been unclear whether an ICL-specific lesion recognition factor exists. We approached this question by biochemical purification of ICL binding affinities from nuclear extracts and identified UHRF1. Previous studies have shown that loss of UHRF1 renders cells sensitive to DNA damage exposure (Jenkins et al., 2005; Muto et al., 2002). In this study, we constructed genetic and knockdown mutants of UHRF1 and analyzed its function in DNA damage response. Our experimental evidence suggests that UHRF1 possesses activities recognizing ICL lesions while also interacting with lesion processing nucleases, suggesting that it is a candidate factor in promoting DNA damage processing.

Author Manuscript Author Manuscript Author Manuscript Author Manuscript

### DNA damage affinity of UHRF1

The lesion-binding ability of UHRF1 was examined by three independent approaches: cell biology with laser-localized ICLs *in vivo*; ChIP-based ICL damage enrichment at the molecular level; and biochemical binding assays *in vitro*. Results from these experiments consistently indicated that UHRF1 exhibited strong and direct affinity toward DNA ICL damage. The structural basis for UHRF1's ICL binding affinity is not clear. Using a panel of UHRF1 domain deletion mutants, we found that the SRA domain is required for the binding to ICL lesions (Figure 2E). The SRA domain has been reported to exhibit a moderate affinity toward hemimethylated CpG duplex DNA and was considered as a hemimethylation recognition mechanism for the recruitment of DNMT1 (Avvakumov et al., 2008). Recent studies, however, indicate that the Tudor and E3 ligase domains play more critical roles in directing DNMT1 to hemimethylated DNA (Arita et al., 2012; Liu et al., 2013; Nishiyama et al., 2013). It is conceivable that the UHRF1 SRA domain exhibits structural flexibility and can recognize a broad range of damage-induced helix distortions, thus enabling it to bind to a variety of damages.

### UHRF1 as a nuclease scaffold

Lack of DNA damage-induced γH2AX and 53BP1 foci accumulation in the UHRF1 mutant cells hinted at an impaired lesion processing which could arise from a deficit of nuclease activity at the site of the lesion. Accordingly, we examined UHRF1 protein-protein interactions and found both ERCC1/XPF and MUS81/EME1 are associated with UHRF1, suggesting that structure-specific endonucleases interact with UHRF1 in their heterodimeric forms. A protein-protein interaction between UHRF1 and EME1 was previously detected by a yeast two-hybrid screen (Mistry et al., 2008). This observation also suggests a direct interaction between UHRF1 and lesion processing enzymes.

The functionality of the interactions is supported by the reduced nuclease recruitment to the sites of DNA lesions. The dual activities of UHRF1 in damage-binding and nuclease association functions may allow it to recruit lesion-processing activities to promote DNA damage removal. Such a property is akin to the NER protein XPA, which has lesion-binding affinity and acts as a scaffold for nuclease recruitment (Li et al., 1994; Orelli et al., 2010). The dual activities of UHRF1 is also functionally analogous to that of budding SAW1 protein which binds flap structures and promotes the recruitment of Rad1/Rad10 through direct interactions (Li et al.).

Interestingly, the nuclease recruitment function of UHRF1 seems non-epistatic to that of SLX4/FANCP. This is supported by the experiments examining DNA damage sensitivity in cells with combined UHRF1 and SLX4 depletions. SLX4 is considered a main downstream effector of FA pathway activation, which is presumed to guide lesion processing and Holliday junction resolution lesion processing nucleases (Hodskinson et al., 2014; Klein Douwel et al., 2014; Wan et al., 2013). The enhanced phenotype from a combined loss of SLX4 and UHRF1 suggests that UHRF1 provides a parallel mechanism for the enrichment of lesion processing nucleases (Figure 5E). Such a notion is further supported by the epistatic analyses indicating that UHRF1 function is non-redundant to FANCL. However, given the early lesion recognition function of UHRF1, it remains possible that a portion of

Author Manuscript Author Manuscript Author Manuscript Author Manuscript

UHRF1 function is projected through promoting FA pathway activation. Together, our findings revealed a DNA damage response function of UHRF1 and an FA pathway independent mechanism of nuclease recruitment to the site of lesions.

## Experimental Procedures

### Antibodies and plasmids

Commercial antibodies used in this study were purchased as follows, anti-human UHRF1 (Abgent NP-037414); anti-γH2AX (Upstate 07-164); anti-human mus81 (Thermo MA1-5837); anti-human ERCC1 (NeoMarker MS-671-P0); anti-MCM5 (Bethyl A300-195A). Wild type UHRF1 cDNA, ΔPHD, ΔSRA, ΔRING constructs in pPyCAGIP-flag vector were a kind gift from Dr. Jiemin Wong's laboratory. pENTER-UHRF1C724A and pENTER-UHRF1H741A were a kind gift from Dr. Yonchu Jenkins (Rigel Pharmaceuticals).

### eChIP assay

The eChIP assay protocol and substrate preparation were described earlier (Shen et al., 2009). Cisplatin-adducted plasmid substrates were prepared by incubating the pOriP plasmid with different dose of cisplatin for 3 hours at 37°C in the dark.

### Clonogenic survival assay

$1–3\times10^5$ cells were seeded in a 100 mm culture plate 24 hours prior to treatment. Cells were exposed to various doses of DNA damage agents for one hour and then seeded with appropriate cell number in triplicates for each dosage. After 14 days, colonies were fixed with 6% glutaraldehyde (v/v) and stained with 0.5% crystal violet (w/v).

## Supplementary Material

Refer to Web version on PubMed Central for supplementary material.

## Acknowledgments

The authors wish to thank Y Jenkins (Rigel Pharmaceuticals) and JM Wong (East China Normal University) for providing critical reagents, and Jia Liu of the Core Facility B (CA097175) for assistance in preparing crosslinked DNA substrates. This work was supported by grants from the NIH (CA097175-Project 3, CA179441, and CA97175 to L.L; CA157448 to J.C.). This research was also supported in part by the Intramural Research Program of the NIH, National Institute on Aging (AG000746-02). JQ is supported by CPRIT/RP110784 and BCM Cancer Center Pathway Discovery core. This work is also supported by the Cancer Center Support Grant (CA016672) and the Hubert L & Olive Stringer endowed professorship to L.L.

## References

Arita K, Isogai S, Oda T, Unoki M, Sugita K, Sekiyama N, Kuwata K, Hamamoto R, Tochio H, Sato M, et al. Recognition of modification status on a histone H3 tail by linked histone reader modules of the epigenetic regulator UHRF1. Proceedings of the National Academy of Sciences of the United States of America. 2012; 109:12950–12955. [PubMed: 22837395]

Avvakumov GV, Walker JR, Xue S, Li Y, Duan S, Bronner C, Arrowsmith CH, Dhe-Paganon S. Structural basis for recognition of hemi-methylated DNA by the SRA domain of human UHRF1. Nature. 2008; 455:822–825. [PubMed: 18772889]

Author Manuscript Author Manuscript Author Manuscript Author Manuscript

Bhagwat N, Olsen AL, Wang AT, Hanada K, Stuckert P, Kanaar R, D'Andrea A, Niedernhofer LJ, McHugh PJ. XPF-ERCC1 Participates in the Fanconi Anemia Pathway of Cross-Link Repair. Molecular and cellular biology. 2009; 29:6427–6437. [PubMed: 19805513]

Bostick M, Kim JK, Estève P-O, Clark A, Pradhan S, Jacobsen SE. UHRF1 Plays a Role in Maintaining DNA Methylation in Mammalian Cells. Science. 2007; 317:1760–1764. [PubMed: 17673620]

D'Andrea AD. Susceptibility pathways in Fanconi's anemia and breast cancer. The New England journal of medicine. 2010; 362:1909–1919. [PubMed: 20484397]

Fekairi S, Scaglione S, Chahwan C, Taylor ER, Tissier A, Coulon S, Dong M-Q, Ruse C, Yates Iii JR, Russell P, et al. Human SLX4 Is a Holliday Junction Resolvase Subunit that Binds Multiple DNA Repair/Recombination Endonucleases. Cell. 2009; 138:78–89. [PubMed: 19596236]

Guervilly J-H, Takedachi A, Naim V, Scaglione S, Chawhan C, Lovera Y, Despras E, Kuraoka I, Kannouche P, Rosselli F, et al. The SLX4 Complex Is a SUMO E3 Ligase that Impacts on Replication Stress Outcome and Genome Stability. Molecular cell. 57:123–137. [PubMed: 25533188]

Hodskinson MR, Silhan J, Crossan GP, Garaycoechea JI, Mukherjee S, Johnson CM, Scharer OD, Patel KJ. Mouse SLX4 is a tumor suppressor that stimulates the activity of the nuclease XPF-ERCC1 in DNA crosslink repair. Molecular cell. 2014; 54:472–484. [PubMed: 24726326]

Hodskinson, Michael RG.; Silhan, J.; Crossan, Gerry P.; Garaycoechea, Juan I.; Mukherjee, S.; Johnson, Christopher M.; Schärer, Orlando D.; Patel, Ketan J. Mouse SLX4 Is a Tumor Suppressor that Stimulates the Activity of the Nuclease XPF-ERCC1 in DNA Crosslink Repair. Molecular cell. 54:472–484. [PubMed: 24726326]

Jenkins Y, Markovtsov V, Lang W, Sharma P, Pearsall D, Warner J, Franci C, Huang B, Huang J, Yam GC, et al. Critical role of the ubiquitin ligase activity of UHRF1, a nuclear RING finger protein, in tumor cell growth. Molecular biology of the cell. 2005; 16:5621–5629. [PubMed: 16195352]

Kim H, D'Andrea AD. Regulation of DNA cross-link repair by the Fanconi anemia/BRCA pathway. Genes & development. 2012; 26:1393–1408. [PubMed: 22751496]

Kim Y, Spitz GS, Veturi U, Lach FP, Auerbach AD, Smogorzewska A. Regulation of multiple DNA repair pathways by the Fanconi anemia protein SLX4. Blood. 2013; 121:54–63. [PubMed: 23093618]

Klein Douwel D, Boonen RA, Long DT, Szypowska AA, Raschle M, Walter JC, Knipscheer P. XPF-ERCC1 acts in Unhooking DNA interstrand crosslinks in cooperation with FANCD2 and FANCP/SLX4. Molecular cell. 2014; 54:460–471. [PubMed: 24726325]

Knipscheer P, Räschle M, Smogorzewska A, Enoiu M, Ho TV, Schärer OD, Elledge SJ, Walter JC. The Fanconi Anemia Pathway Promotes Replication-Dependent DNA Interstrand Cross-Link Repair. Science. 2009; 326:1698–1701. [PubMed: 19965384]

Li F, Dong J, Pan X, Oum J-H, Boeke JD, Lee SE. Microarray-Based Genetic Screen Defines SAW1, a Gene Required for Rad1/Rad10-Dependent Processing of Recombination Intermediates. Molecular cell. 30:325–335. [PubMed: 18471978]

Li L, Elledge SJ, Peterson CA, Bales ES, Legerski RJ. Specific association between the human DNA repair proteins XPA and ERCC1. Proceedings of the National Academy of Sciences of the United States of America. 1994; 91:5012–5016. [PubMed: 8197174]

Liu X, Gao Q, Li P, Zhao Q, Zhang J, Li J, Koseki H, Wong J. UHRF1 targets DNMT1 for DNA methylation through cooperative binding of hemi-methylated DNA and methylated H3K9. Nat Commun. 2013; 4(1563)

Long DT, Räschle M, Joukov V, Walter JC. Mechanism of RAD51-Dependent DNA Interstrand Cross-Link Repair. Science. 2011; 333:84–87. [PubMed: 21719678]

McHugh PJ, Spanswick VJ, Hartley JA. Repair of DNA interstrand crosslinks: molecular mechanisms and clinical relevance. The lancet oncology. 2001; 2:483–490. [PubMed: 11905724]

Mistry H, Gibson L, Yun JW, Sarras H, Tamblyn L, McPherson JP. Interplay between Np95 and Eme1 in the DNA damage response. Biochemical and Biophysical Research Communications. 2008; 375:321–325. [PubMed: 18692478]

Author Manuscript Author Manuscript Author Manuscript Author Manuscript

Muniandy PA, Thapa D, Thazhathveetil AK, Liu ST, Seidman MM. Repair of laser-localized DNA interstrand cross-links in G1 phase mammalian cells. The Journal of biological chemistry. 2009; 284:27908–27917. [PubMed: 19684342]

Muñoz IM, Hain K, Déclais A-C, Gardiner M, Toh GW, Sanchez-Pulido L, Heuckmann JM, Toth R, Macartney T, Eppink B, et al. Coordination of Structure-Specific Nucleases by Human SLX4/BTBD12 Is Required for DNA Repair. Molecular cell. 2009; 35:116–127. [PubMed: 19595721]

Munoz IM, Hain K, Declais AC, Gardiner M, Toh GW, Sanchez-Pulido L, Heuckmann JM, Toth R, Macartney T, Eppink B, et al. Coordination of structure-specific nucleases by human SLX4/BTBD12 is required for DNA repair. Molecular cell. 2009; 35:116–127. [PubMed: 19595721]

Muto M, Kanari Y, Kubo E, Takabe T, Kurihara T, Fujimori A, Tatsumi K. Targeted Disruption of Np95 Gene Renders Murine Embryonic Stem Cells Hypersensitive to DNA Damaging Agents and DNA Replication Blocks. Journal of Biological Chemistry. 2002; 277:34549–34555. [PubMed: 12084726]

Nishiyama A, Yamaguchi L, Sharif J, Johmura Y, Kawamura T, Nakanishi K, Shimamura S, Arita K, Kodama T, Ishikawa F, et al. Uhrf1-dependent H3K23 ubiquitylation couples maintenance DNA methylation and replication. Nature. 2013; 502:249–253. [PubMed: 24013172]

Orelli B, McClendon TB, Tsodikov OV, Ellenberger T, Niedernhofer LJ, Scharer OD. The XPA-binding domain of ERCC1 is required for nucleotide excision repair but not other DNA repair pathways. The Journal of biological chemistry. 2010; 285:3705–3712. [PubMed: 19940136]

Ouyang J, Garner E, Hallet A, Nguyen Hai D, Rickman Kimberly A, Gill G, Smogorzewska A, Zou L. Noncovalent Interactions with SUMO and Ubiquitin Orchestrate Distinct Functions of the SLX4 Complex in Genome Maintenance. Molecular cell. 57:108–122. [PubMed: 25533185]

Sarkar S, Davies AA, Ulrich HD, McHugh PJ. DNA interstrand crosslink repair during G1 involves nucleotide excision repair and DNA polymerase zeta. Embo J. 2006; 25:1285–1294. [PubMed: 16482220]

Shen X, Do H, Li Y, Chung WH, Tomasz M, de Winter JP, Xia B, Elledge SJ, Wang W, Li L. Recruitment of fanconi anemia and breast cancer proteins to DNA damage sites is differentially governed by replication. Molecular cell. 2009; 35:716–723. [PubMed: 19748364]

Smogorzewska A, Desetty R, Saito TT, Schlabach M, Lach FP, Sowa ME, Clark AB, Kunkel TA, Harper JW, Colaiácovo MP, et al. A Genetic Screen Identifies FAN1, a Fanconi Anemia-Associated Nuclease Necessary for DNA Interstrand Crosslink Repair. Molecular cell. 2010; 39:36–47. [PubMed: 20603073]

Stoepker C, Hain K, Schuster B, Hilhorst-Hofstee Y, Rooimans MA, Steltenpool J, Oostra AB, Eirich K, Korthof ET, Nieuwint AWM, et al. SLX4, a coordinator of structure-specific endonucleases, is mutated in a new Fanconi anemia subtype. Nature genetics. 2011; 43:138–141. [PubMed: 21240277]

Svendsen JM, Smogorzewska A, Sowa ME, O'Connell BC, Gygi SP, Elledge SJ, Harper JW. Mammalian BTBD12/SLX4 Assembles A Holliday Junction Resolvase and Is Required for DNA Repair. Cell. 2009; 138:63–77. [PubMed: 19596235]

Wan B, Yin J, Horvath K, Sarkar J, Chen Y, Wu J, Wan K, Lu J, Gu P, Yu EY, et al. SLX4 assembles a telomere maintenance toolkit by bridging multiple endonucleases with telomeres. Cell reports. 2013; 4:861–869. [PubMed: 24012755]

Wang AT, Sengerova B, Cattell E, Inagawa T, Hartley JM, Kiakos K, Burgess-Brown NA, Swift LP, Enzlin JH, Schofield CJ, et al. Human SNM1A and XPF-ERCC1 collaborate to initiate DNA interstrand cross-link repair. Genes & development. 2011; 25:1859–1870. [PubMed: 21896658]

Williams, Hannah L.; Gottesman, Max E.; Gautier, J. Replication-Independent Repair of DNA Interstrand Crosslinks. Molecular cell. 2012; 47:140–147. [PubMed: 22658724]

Yamamoto KN, Kobayashi S, Tsuda M, Kurumizaka H, Takata M, Kono K, Jiricny J, Takeda S, Hirota K. Involvement of SLX4 in interstrand cross-link repair is regulated by the Fanconi anemia pathway. Proceedings of the National Academy of Sciences of the United States of America. 2011; 108:6492–6496. [PubMed: 21464321]

Yan Z, Guo R, Paramasivam M, Shen W, Ling C, Fox D 3rd, Wang Y, Oostra AB, Kuehl J, Lee DY, et al. A ubiquitin-binding protein, FAAP20, links RNF8-mediated ubiquitination to the Fanconi anemia DNA repair network. Molecular cell. 2012; 47:61–75. [PubMed: 22705371]

Author Manuscript Author Manuscript Author Manuscript Author Manuscript

Zheng H, Wang X, Warren AJ, Legerski RJ, Nairn RS, Hamilton JW, Li L. Nucleotide excision repair- and polymerase eta-mediated error-prone removal of mitomycin C interstrand cross-links. Molecular and cellular biology. 2003; 23:754–761. [PubMed: 12509472]

Author Manuscript Author Manuscript Author Manuscript Author Manuscript

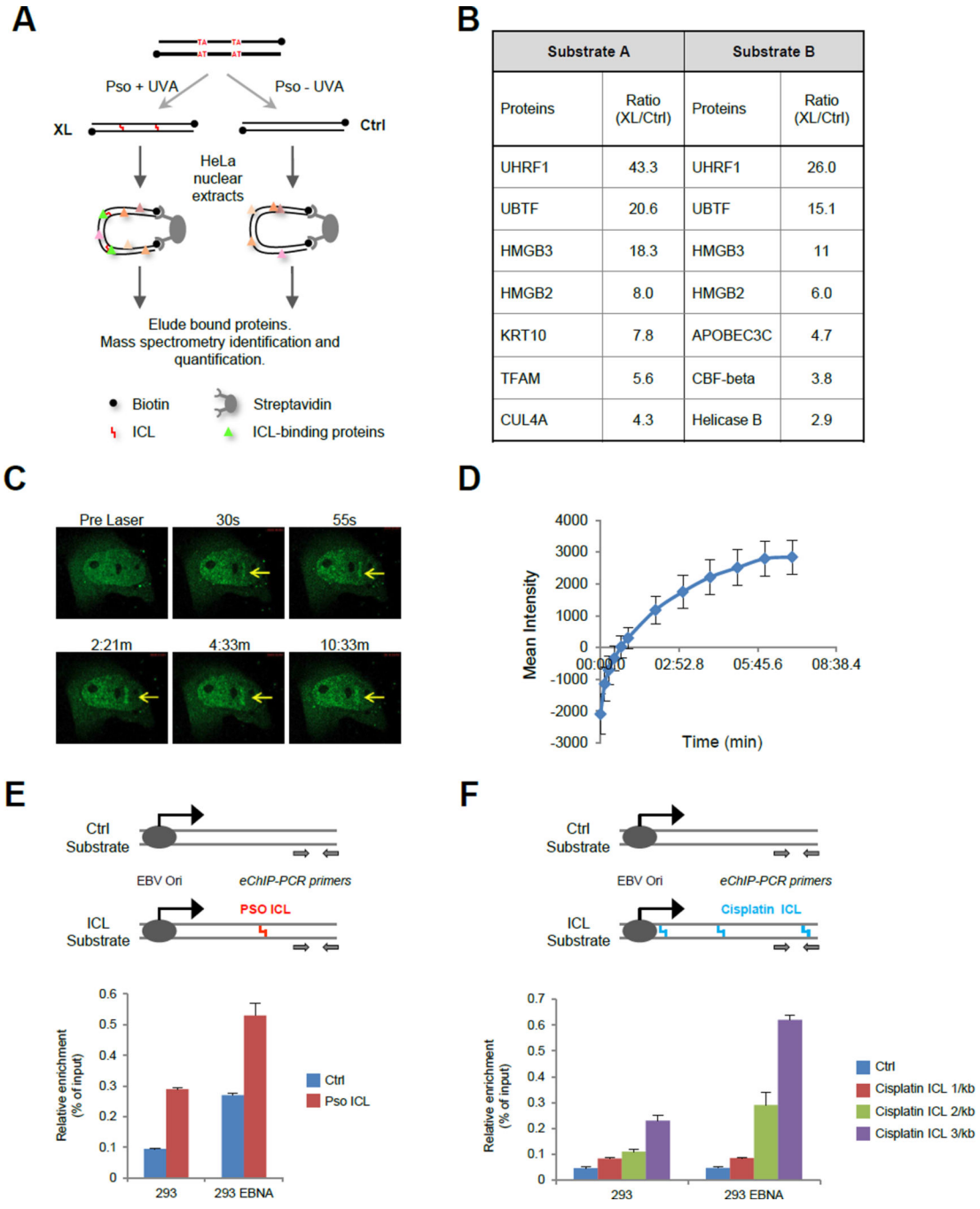


| Substrate A | | Substrate B | |
|---|---|---|---|
| Proteins | Ratio (XL/Ctrl) | Proteins | Ratio (XL/Ctrl) |
| UHRF1 | 43.3 | UHRF1 | 26.0 |
| UBTF | 20.6 | UBTF | 15.1 |
| HMGB3 | 18.3 | HMGB3 | 11 |
| HMGB2 | 8.0 | HMGB2 | 6.0 |
| KRT10 | 7.8 | APOBEC3C | 4.7 |
| TFAM | 5.6 | CBF-beta | 3.8 |
| CUL4A | 4.3 | Helicase B | 2.9 |

**Figure 1. Identification of UHRF1 as an ICL-interacting protein**

(**A**) A schematic of pulldown/mass spectrometry-based purification of ICL-binding proteins. The 120-bp crosslinked substrate contains two psoralen ICLs at defined positions and is end-labeled with Biotin for the pulldown assay.

(**B**) Candidate ICL-binding proteins identified by mass spectrometry analyses using two independent ICL-containing DNA substrates.

(**C**) Time-laps images showing recruit of GFP-tagged UHRF1 to laser-localized psoralen ICLs in U2OS cell nuclei at indicated time points.

Author Manuscript Author Manuscript Author Manuscript Author Manuscript

(**D**) Imaging quantification of nuclear strip intensity of GFP-tagged UHRF1 to laser-localized psoralen ICLs in U2OS cells.
(**E**) *Top panel*: Schematic representation of the DNA substrate used in the eChIP assay. The presence of a single-defined psoralen-ICL is indicated. The arrow indicates the direction of replication fork movement. Small arrows indicate the region of Q-PCR amplification. *Bottom panel*: eChIP assay measuring the recruitment of the UHRF1 protein in 293 and 293EBNA cells. Error bars represent standard deviations from four independent experiments.
(**F**) *Top panel*: Schematic representation of the DNA substrates used in the eChIP assay. The presence of random cisplatin-ICLs is illustrated. Small arrows indicate the region of Q-PCR amplification. *Bottom panel*: eChIP assay measuring the recruitment of the UHRF1 protein in 293 and 293EBNA cells. Numbers of cisplatin ICL per kb represent average distributions. Error bars represent standard deviations from three independent experiments.

Author Manuscript Author Manuscript Author Manuscript Author Manuscript

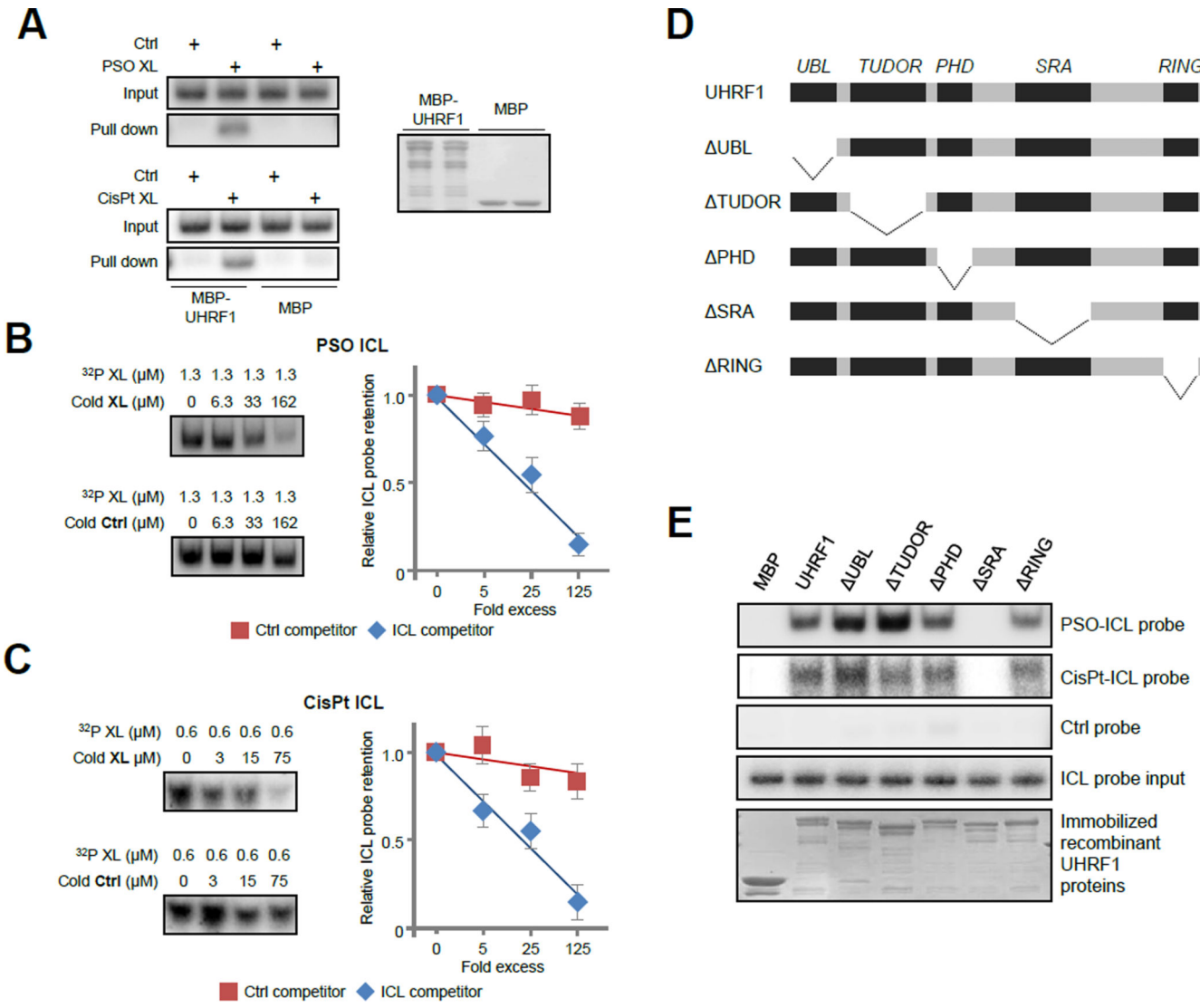


**Figure 2. UHRF1 binds to ICLs directly to ICLs through the SRA domain**

(**A**) Binding of MBP-tagged UHRF1 to crosslinked (XL) and control (Ctrl) probes with $^{32}$P end-labeling (*left panels*). MBP or MBP-UHRF1 were immobilized onto amylose beads and incubated with PSO ICL- or cisplatin ICL-containing probes. Bound DNA was eluded with maltose, and resolved on 2% agarose gel. Aliquots of amylose beads bound proteins were eluded and resolved by PAGE as the loading control (*Right panel*).

(**B**) Binding affinity of UHRF1 toward psoralen DNA ICL. *Left panel*: MBP-tagged UHRF1 was preincubated with $^{32}$P-labeled PSO-ICL probe prior to the addition of cold PSO-ICL competitor probe (Top) or cold control competitor probe (bottom), with the indicated concentrations. Bound DNA was recovered by amylose beads and resolved on 2% agarose gel to reveal the retention of $^{32}$P-labeled PSO-ICL probe. *Right panel*: quantification of relative ICL retention as a function of excess amount of control or ICL competitors. Error bars represent standard deviations from three independent experiments.

(**C**) Binding affinity of UNRF1 toward cisplatin DNA ICL, performed as in (B).

Author Manuscript Author Manuscript Author Manuscript Author Manuscript

(**D**) Illustration of UHRF1 domain structure and UHRF1 domain deletion mutants. UBL, ubiquitin-like domain; TUDOR, tandem tudor domain; PHD, plant homeodomain; SRA, SET and RING-associated domain; RING, really interesting new gene domain.
(**E**) Binding of UHRF1 domain deletion mutants to PSO-ICL and cisplatin-ICL probes. *Bottom panel*: input recombinant proteins for the ICL binding assay as performed in (A).

Author Manuscript Author Manuscript Author Manuscript Author Manuscript

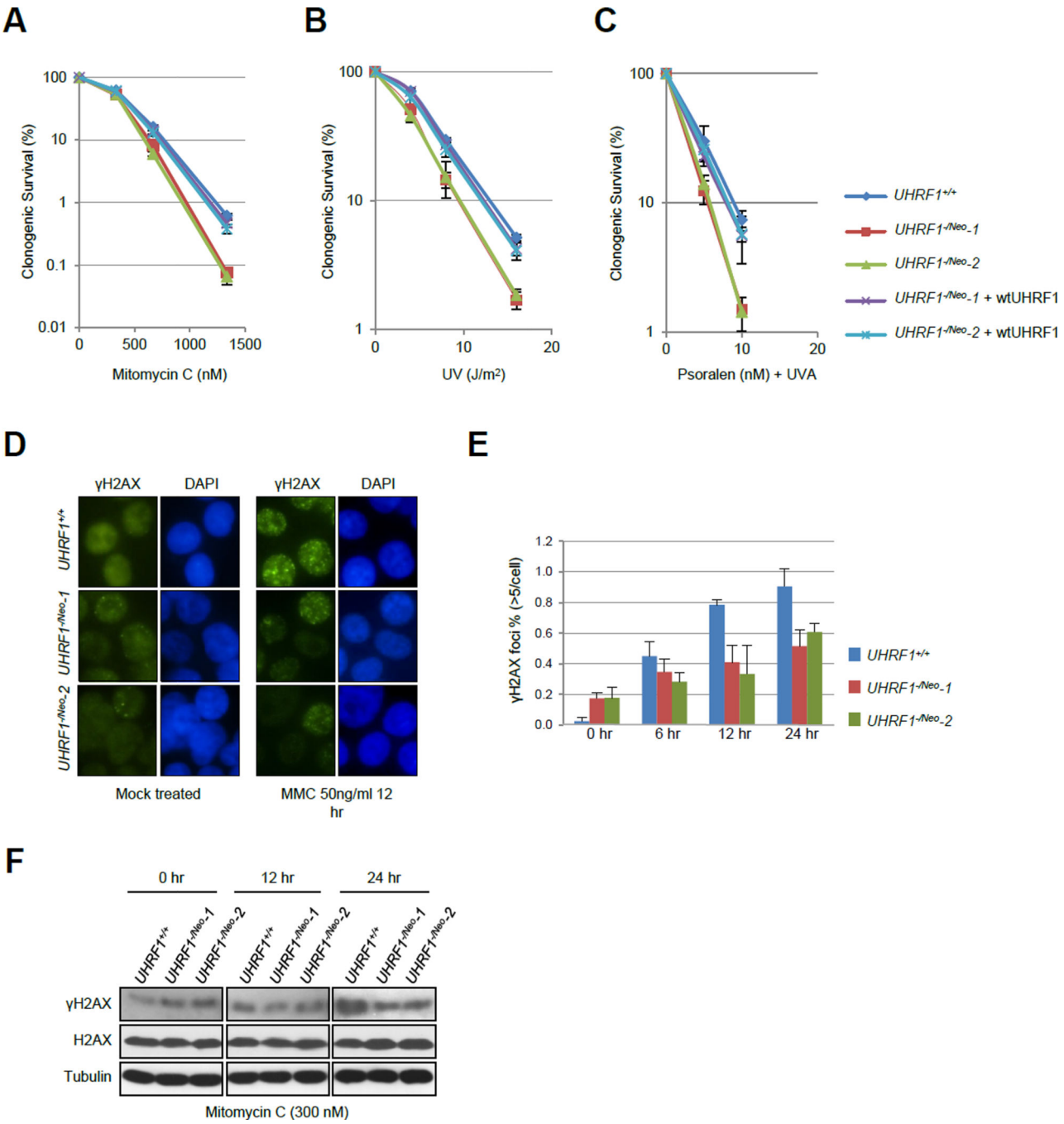


**Figure 3. UHRF1 deficiency sensitizes cells to DNA damage and attenuates lesion processing**

Clonogenic survival of *UHRF1*$^{-/Neo}$*-1* and *UHRF1*$^{-/Neo}$*-2* and their complemented derivatives exposed to (**A**) mitomycin C, (**B**) UV, and (**C**) psoralen plus UVA treatment. Error bars represent SD across three or more technical replicates.

(**D**) Formation of MMC-induced γH2AX nuclear foci in wild type (*UHRF1*$^{+/+}$) and hypomorphic mutant (*UHRF1*$^{-/Neo}$*-1* and *UHRF1*$^{-/Neo}$*-2*) cells 12 hours after treatment.

(**E**) Percentage of γH2AX foci-positive nuclei from MMC-treated *UHRF1*$^{+/+}$ and *UHRF1*$^{-/Neo}$*-1* and *UHRF1*$^{-/Neo}$*-2* cells at indicated time points after MMC exposure.

(**F**) Immunoblot detecting γH2AX in *UHRF1*$^{+/+}$ and *UHRF1*$^{-/Neo}$ cells treated with mitomycin C and collected at indicated time points.

Author Manuscript Author Manuscript Author Manuscript Author Manuscript

Author Manuscript Author Manuscript Author Manuscript Author Manuscript

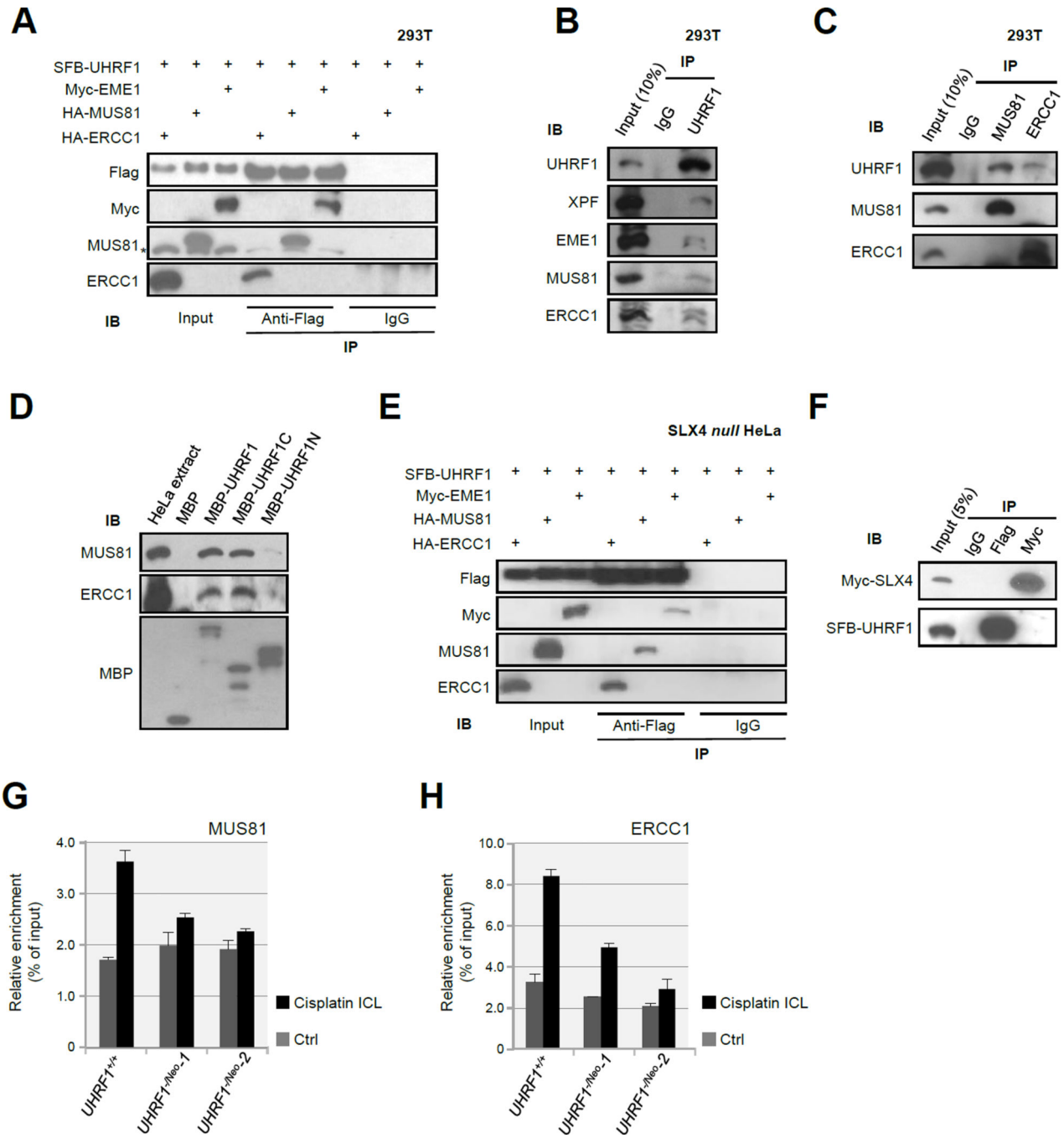


**Figure 4. UHRF1-dependent recruitment of ICL-processing nucleases**

(**A**) Co-immunoprecipation between UHRF1 and ICL processing nucleases. 293T cells co-transfected with SFB-tagged UHRF1 and indicated nucleases were co-immunoprecipitated with anti-Flag antibody and immunoblotted (IB) with indicated antibodies. The asterisk marks a nonspecific band in 293 cells.

(**B**) Immunoblot detecting indicated proteins from control (IgG) and UHRF1 co-immunoprecipitation of MMC-treated 293T cells.

Author Manuscript Author Manuscript Author Manuscript Author Manuscript

(**C**) Immunoblot detecting UHRF1 from control (IgG), MUS81, and ERCC1 antibody co-immunoprecipitation of MMC-treated 293T cells.

(**D**) Pull down of MUS81 and ERCC1 from HeLa extract. MBP-UHRF1 and two UHRF1 truncations, UHRF1C (ΔUBL-TUDOR-PHD) and MBP-UHRF1N (ΔSRA-RING) were immobilized onto amylose beads and incubated with HeLa nuclear extract. Bound proteins were eluted with maltose for immunoblot detection of ERCC1 and MUS81.

(**E**) Co-immunoprecipation between UHRF1 and ICL processing nucleases. SLX4-*null* HeLa cells co-transfected with SFB-tagged UHRF1 and indicated nucleases were in co-immunoprecipitation with anti-Flag antibody as immunoblotted (IB) with indicated antibodies.

(**F**) Reciprocal immunoprecipation between UHRF1 and SLX4. 293T cells co-transfected with SFB-tagged UHRF1 and Myc-tagged SLX4 were subjected to reciprocal IP with anti-Myc and anti-Flag antibodies.

(**G**) eChIP assay measuring the recruitment of Mus81 to cisplatin ICLs in $UHRF1^{+/+}$, $UHRF1^{-/Neo}$-*1*, and $UHRF1^{-/Neo}$-*2* cells. Error bars represent SDs derived from three independent experiments.

(**H**) eChIP assay measuring the recruitment of ERCC1 to cisplatin ICLs in $UHRF1^{+/+}$, $UHRF1^{-/Neo}$-*1*, and $UHRF1^{-/Neo}$-*2* cells. Error bars represent SDs derived from three independent experiments.

Author Manuscript Author Manuscript Author Manuscript Author Manuscript

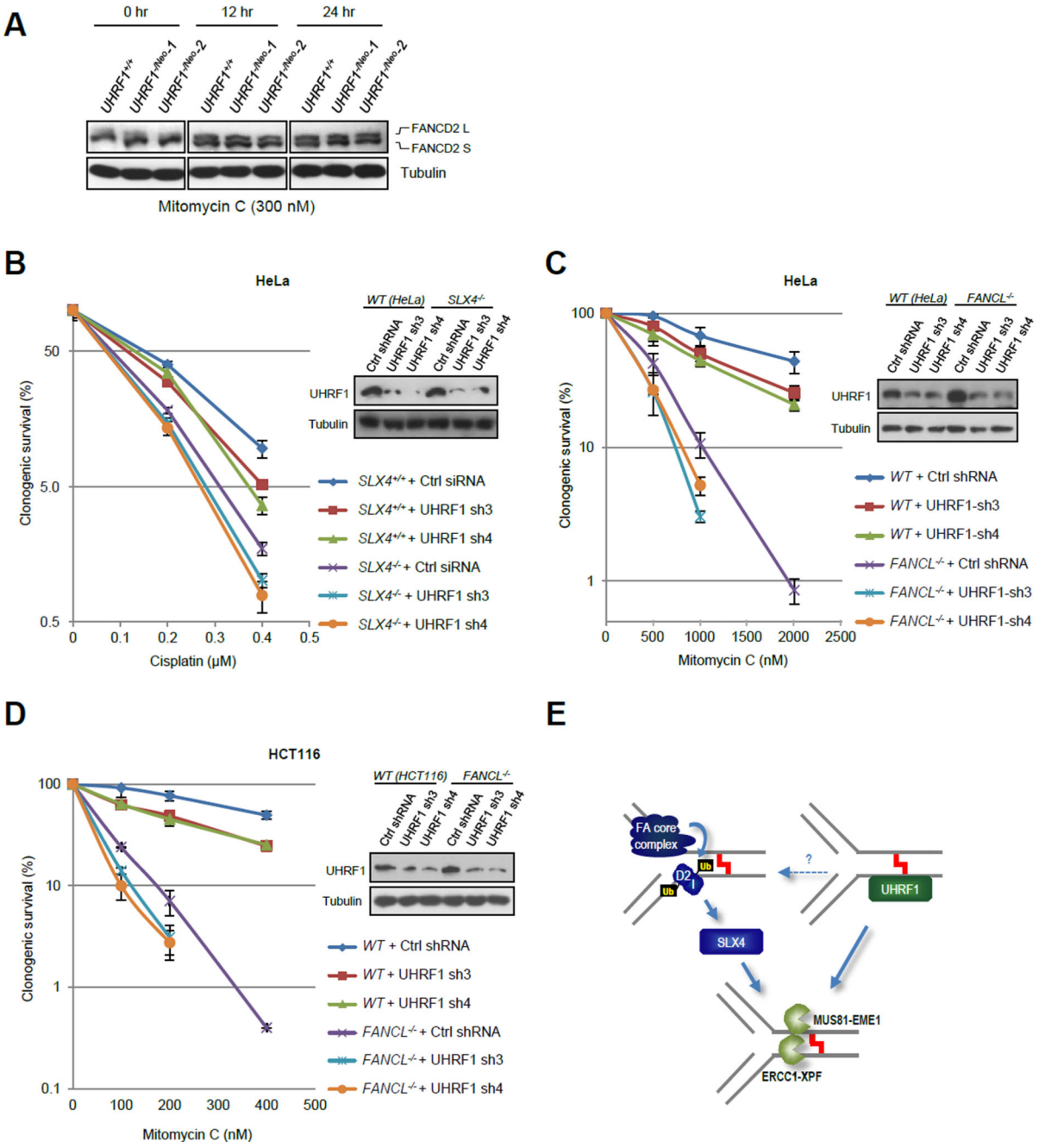


**Figure 5. UHRF1-dependent recruitment of ICL-processing nucleases**

(**A**) Co-immunoprecipation between UHRF1 and ICL processing nucleases. 293T cells co-transfected with SFB-tagged UHRF1 and indicated nucleases were co-immunoprecipitated with anti-Flag antibody and immunoblotted (IB) with indicated antibodies. The asterisk marks a nonspecific band in 293 cells.

(**B**) Immunoblot detecting indicated proteins from control (IgG) and UHRF1 co-immunoprecipitation of MMC-treated 293T cells.

Author Manuscript Author Manuscript Author Manuscript Author Manuscript

(**C**) Immunoblot detecting UHRF1 from control (IgG), MUS81, and ERCC1 antibody co-immunoprecipitation of MMC-treated 293T cells.

(**D**) Pull down of MUS81 and ERCC1 from HeLa extract. MBP-UHRF1 and two UHRF1 truncations, UHRF1C (ΔUBL-TUDOR-PHD) and MBP-UHRF1N (ΔSRA-RING) were immobilized onto amylose beads and incubated with HeLa nuclear extract. Bound proteins were eluted with maltose for immunoblot detection of ERCC1 and MUS81.

(**E**) Co-immunoprecipation between UHRF1 and ICL processing nucleases. SLX4-*null* HeLa cells co-transfected with SFB-tagged UHRF1 and indicated nucleases were in co-immunoprecipitation with anti-Flag antibody as immunoblotted (IB) with indicated antibodies.

(**F**) Reciprocal immunoprecipation between UHRF1 and SLX4. 293T cells co-transfected with SFB-tagged UHRF1 and Myc-tagged SLX4 were subjected to reciprocal IP with anti-Myc and anti-Flag antibodies.

(**G**) eChIP assay measuring the recruitment of Mus81 to cisplatin ICLs in $UHRF1^{+/+}$, $UHRF1^{-/Neo}$-*1*, and $UHRF1^{-/Neo}$-*2* cells. Error bars represent SDs derived from three independent experiments.

(**H**) eChIP assay measuring the recruitment of ERCC1 to cisplatin ICLs in $UHRF1^{+/+}$, $UHRF1^{-/Neo}$-*1*, and $UHRF1^{-/Neo}$-*2* cells. Error bars represent SDs derived from three independent experiments.

Author Manuscript Author Manuscript Author Manuscript Author Manuscript

**Figure 7. UHRF1 has non-redundant function to the FA pathway in ICL DNA damage response**

(**A**) Immunoblots detecting FANCD2 monoubiquitination in cells with indicated genotypes treated or mock-treated with MMC (300 ng/ml). L and S represent monoubiquitinated and native forms of FANCD2, respectively. Note that the Tubulin loading control is shared with Fig. 5C as they are from the same blot.

(**B**) Clonogenic survival of *SLX4*$^{-/-}$ HeLa cells infected with lentivirus expressing control (Ctrl) or UHRF1 shRNA (sh3 and sh4).

(**C**) Clonogenic survival of *FANCL*$^{-/-}$ HeLa cells with UHRF1 knockdown (UHRF1 sh3 and sh4).

(**D**) Clonogenic survival of HCT116 (WT) and *FANCL*$^{-/-}$ HCT116 cells with UHRF1 knockdown (UHRF1 sh3 and sh4).

(**E**) A model depicting UHRF1 as a damage sensor and nuclease scaffold parallel to the FA-SLX4-mediated ICL DNA damage response.